Review of ground temperatures in the Mallik field area: a constraint to the methane hydrate stability

J.A. Majorowicz[1] and S.L. Smith[2]

Majorowicz, J.A. and Smith, S.L., 1999: Review of ground temperatures in the Mallik field area: a constraint to the methane hydrate stability; in *Scientific Results from JAPEX/JNOC/GSC Mallik 2L-38 Gas Hydrate Research Well, Mackenzie Delta, Northwest Territories, Canada, (ed.) S.R. Dallimore, T. Uchida, and T.S. Collett; Geological Survey of Canada, Bulletin 544, p. 45–56.*

Abstract: Analysis of data from 32 industrial exploration wells in the Mallik field and surrounding area in the Mackenzie Delta–Beaufort Sea region allowed construction of temperature-depth profiles using regional heat-flow values, temperature at the base of ice-bearing permafrost, and models of thermal conductivity with depth. An analysis of the stability conditions for methane hydrate showed that it is stable in the Mallik field area and that the depth to the base of the methane hydrate stability zone can be as deep as 1500 ± 100 m in areas of thick permafrost. The depth to the base of the methane hydrate stability zone, calculated in this study using reconstructed temperature-depth profiles, was found in a majority of the wells to be 50–150 m deeper than that previously determined using linear temperature profiles and a constant thermal conductivity with depth.

Résumé : L'analyse de données provenant de 32 puits d'exploration forés dans le champ de Mallik et les environs dans la région du delta du Mackenzie et de la mer de Beaufort a permis d'établir des profils de température-profondeur basés sur les valeurs du flux thermique régional, sur la température à la base du pergélisol renfermant de la glace et sur les modèles de conductivité thermique en fonction de la profondeur. Une analyse des conditions de stabilité de l'hydrate de méthane a révélé que l'hydrate de méthane est stable dans la région du champ de Mallik et que la profondeur jusqu'à la base de la zone de stabilité de l'hydrate de méthane peut atteindre 1 500 ± 100 m aux endroits où le pergélisol est épais. Dans la majorité des puits, la profondeur jusqu'à la base de la zone de stabilité de l'hydrate de méthane calculée en utilisant des profils reconstruits de température-profondeur est de 50 à 150 m de plus que ce qui a été déterminé auparavant en utilisant des profils linéaires de température et une valeur constante de la conductivité thermique en fonction de la profondeur.

[1] Northern Geothermal Consultants, 105 Carlson Close, Edmonton, Alberta, Canada T6R 2J8
[2] Geological Survey of Canada, 601 Booth Street, Ottawa, Ontario, Canada K1A 0E8

INTRODUCTION

The recent discovery of gas hydrate in the Mallik 2L-38 gas hydrate research well (Dallimore and Collett, 1998; Collett and Dallimore, 1998) has renewed interest in the geothermal regime of the Mallik field and the surrounding area (Fig. 1). Majorowicz et al. (1990) used deep temperature data for ten wells in the Mackenzie Delta–Beaufort Sea area to determine the local geothermal gradient and to estimate heat flow. Temperature-depth profiles were also reconstructed for the same ten wells using estimates of heat-flow and average thermal-conductivity values assigned to each stratigraphic unit. A comparison of these reconstructed profiles with observed temperatures indicated that shallow (upper 1 km) industrial borehole temperature data are higher than expected, probably as a result of thermal disturbance from drilling. Majorowicz et al. (1990) concluded that temperature-depth profile reconstructions, constrained by the temperature at the base of ice-bearing permafrost, as well as regional heat-flow and thermal-conductivity data, are needed for more reliable geothermal assessments. A regional geothermal field study based on 188 wells in the Mackenzie Delta–Beaufort Sea region was summarized in Majorowicz et al. (1995). The approach recommended in Majorowicz et al. (1990) is the basis for the analytical method used in this paper to reconstruct the temperature field for 32 of the above 188 wells located in the broad Mallik field area (Table 1), and for which deep temperature data were available.

Figure 1. *Locations of the wells in the Mallik field and surrounding area.*

Gas hydrate has been interpreted from well-log data (mainly resistivity and acoustic logs) to occur in the Mallik field and surrounding area (reported *in* Smith and Judge (1993); Judge et al. (1994)). Judge and Majorowicz (1992) analyzed the stability conditions for methane hydrate in the Mackenzie Delta–Beaufort Sea region. Deep temperature data from industrial exploration wells were used to determine a linear thermal gradient below the base of ice-bearing permafrost and the base of the methane hydrate stability zone. The thickness of the gas hydrate stability zone, calculated assuming this linear temperature gradient, is considered to be a first approximation. The present study uses the reconstructed temperature-depth profiles to determine the base of the methane hydrate stability zone at each well site. This is considered an improvement of the technique used by Judge and Majorowicz (1992) because variations in thermal conductivity with depth are considered. The results of this work can, therefore, be used to refine estimates of the areal and vertical extent of the gas hydrate stability zone as well as estimates of the size of the gas hydrate reservoir.

Table 1. Summary of data for wells in the Mallik field and surrounding area.

Well	Long. (°W)	Lat. (°N)	Grad T (K/km) ± 2 K/km	Heat flow (mW/m^2)	Base ice-bearing permafrost (m)	Base gas hydrate stability zone[1] (m)	Base gas hydrate stability[2] (m) ± 100 m	Approximate thickness stability zone[3] (m)
ARNAK L-30*	133.87	69.83	34	52 ± 8	662	1050 ± 100	1200	980
GARRY P-04*	135.51	69.40	32	58 ± 9	502	950 ± 50	1000	780
GARRY P-07*	135.52	69.44	30	48 ± 7	422	850 ± 50	1000	780
IMMERK B-48*	135.18	69.62	34	55 ± 8	542	950 ± 100	1000	780
ISSERK E-27*	134.37	69.94	30	51 ± 8	674	1200 ± 150	1300	1080
IVIK N-17	134.32	69.61	27	46 ± 7	672	1300 ± 150	1300	1080
IVIK J-26	134.34	69.60	24	47 ± 7	500	1350 ± 50	1200	980
IVIK C-52	134.48	69.52	27	45 ± 7	649	1300 ± 150	1300	1080
IVIK J-54	134.48	69.56	27	43 ± 6	668	1300 ± 50	1200	980
KILAGMIOTAK F-48	134.20	69.46	30	48 ± 7	716	1300 ± 150	1300	1080
KILAGMIOTAK M-16	134.07	69.43	30	46 ± 7	740	1300 ± 150	1200	980
KUGMALLIT H-54*	133.46	69.64	27	45 ± 7	690	1300 ± 150	1400	1180
MALLIK A-06	134.50	69.42	31	55 ± 8	640	1150 ± 50	1300	1080
MALLIK J-37	134.64	69.44	36	49 ± 7	622	1050 ± 100	1300	1080
MALLIK L-38	134.66	69.46	36	55 ± 8	613	1020 ± 150	1100	880
MALLIK P-59	134.71	69.48	28	43 ± 6	645	1250 ± 150	1200	980
NIGLINTGAK H-30*	135.34	69.32	34	61 ± 9	146	unstable	unstable	0
NUKTAK C-22	134.86	69.69	27	39 ± 6	701	1350 ± 50	1500	1280
PELLY B-35*	135.39	69.57	26	44 ± 6	451	1000 ± 150	1100	880
PULLEN E-17*	134.33	69.77	28	47 ± 7	604	1150 ± 50	1200	980
TAGLU P-03*	135.01	69.38	32	53 ± 8	482	900 ± 100	900	680
TAGLU G-33	134.89	69.37	32	55 ± 8	543	1000 ± 50	1100	880
TAGLU C-42	134.94	69.35	30	47 ± 7	600	1100 ± 50	1100	880
TAGLU F-43	134.95	69.37	30	50 ± 8	620	1150 ± 100	1200	980
TAGLU H-54	134.97	69.39	33	45 ± 7	533	950 ± 50	1100	880
TAGLU D-55	134.99	69.40	30	52 ± 8	530	1000 ± 50	1100	880
UMIAK N-10	134.27	69.50	30	51 ± 7	701	1300 ± 50	1400	1180
UMIAK J-37	134.39	69.44	28	51 ± 7	669	1250 ± 150	1300	1080
UNARK 24-A	134.62	69.56	28	50 ± 8	649	1250 ± 50	1400	1180
UPLUK C-21*	135.36	69.33	32	61 ± 9	233	450 ± 50	400	180
UPLUK M-38*	135.41	69.47	28	46 ± 7	409	900 ± 50	900	680
UPLUK A-42*	135.43	69.35	28	34 ± 5	67	unstable	unstable	0

Grad T = geothermal gradient
* Wells outside mapped area shown in Figure 1
[1] Values calculated using linear temperature profile (Judge and Majorowicz, 1992)
[2] Values calculated using reconstructed temperature-depth profiles (from equation 3)
[3] Values calculated using 220 m for top of stability zone and base of stability zone determined using reconstructed temperature-depth profiles

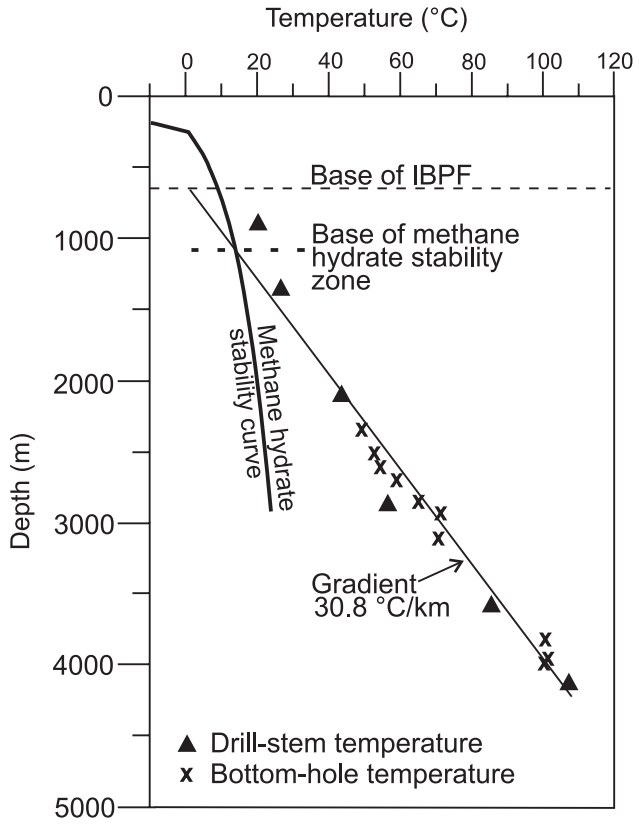

Figure 2. *Linear temperature-depth profile for the Mallik A-06 well in the Mallik field area, determined by applying a least-squares fit to the deep temperature data, superimposed on the methane hydrate stability curve. The area to the left of the stability curve represents conditions for gas hydrate stability. Base of IBPF refers to the base of the ice-bearing permafrost.*

GEOTHERMAL FIELD

Geothermal gradient

Deep temperature data from industrial exploration wells were the primary source of information for this analysis. Bottom-hole-temperature and drill-stem-temperature data were available for depths up to 4250 m for 32 wells in the Mallik field and its vicinity. These data however, generally do not represent the true formation temperatures because circulation of mud in the well during drilling disturbs the temperature in the surrounding rock. If successive temperature measurements are made at the same depth at different times following the cessation of fluid circulation and if the circulation time is known, the equilibrium formation temperature may be estimated using the Horner plot method (*see* Majorowicz et al., 1990; Judge and Majorowicz, 1992).

The temperature data corrected by the Horner method were used to determine the geothermal gradient. Majorowicz et al. (1990) found that industrial temperature records at depths greater than 1500 m generally exhibited a linear relationship with depth. This relationship is shown in Figure 2 for the Mallik A-06 well for which there was a large amount of industrial data available.

For each well, a linear temperature gradient was established between the deep borehole data and the temperature at the base of ice-bearing permafrost using a least-squares fit (Judge and Majorowicz, 1992). The depth to the base of ice-bearing permafrost was determined from petrophysical (downhole) well logs (D&S Petrophysical Consultants, 1983; Thurber Consultants Ltd., unpub. report, 1986, 1988). The temperature at the base of ice-bearing permafrost usually differs from that at the base of permafrost (defined as 0°C) due to the freezing point depression resulting from pressure as well as chemical and soil particle effects. A comparison of well-log picks of the base of ice-bearing permafrost with precision temperature logs in the Mackenzie Delta–Beaufort Sea area (Taylor and Judge, 1981; Taylor et al., 1982) indicates that the temperature at the base of ice-bearing permafrost is approximately -1°C. For the present study, the temperature at the base of ice-bearing permafrost is thus assumed to be -1°C. The geothermal gradient determined for each well is given in Table 1.

The point geothermal gradient data were interpolated using a weighted moving average technique to produce a map (Fig. 3) showing the spatial variation of the geothermal gradient in the Mallik field area and its vicinity. Although only a limited number of wells (19) around the Mallik field is shown on the map, data from outside the mapped area (Table 1) were also used in the interpolation. Considering the error of the geothermal gradient estimate (assessed to be ±2 K/km), the regional variations in geothermal gradient are relatively small and range from 24 K/km to 36 K/km which is typical for most of the Mackenzie Delta–Beaufort Sea area (Majorowicz et al., 1995).

Heat flow

Heat flow may be calculated from the equation for steady-state heat conduction in one dimension:

$$Q = -k(dT/dz) \quad (1)$$

where Q = steady heat flow (W/m^2), k = thermal conductivity ($W/m \cdot K$), and dT/dz = geothermal gradient (K/m), and where T is the temperature and z is the depth.

Due to the large effort and uncertainties involved in establishing measured thermal conductivities for all places within a wide area, a method of estimating thermal conductivity from 'net-rock' data is normally used (Majorowicz et al., 1995). In this method, a thermal-conductivity value for each rock type in the sedimentary section is assumed. These values are then used with the lithological and stratigraphic information in the form of a net rock analysis for each formation or for

different depth intervals through the section. An effective thermal conductivity (k_f) can be evaluated for the entire sedimentary sequence according to the series model (Majorowicz et al., 1990):

$$k_f = \frac{\sum_i l_i}{\sum_i \frac{l_i}{k_i}} \qquad (2)$$

where l_i is the fractional content of the i-th rock type and k_i is the thermal conductivity of that rock type. This method represents a reasonable option for regional geothermal mapping. It is expected that the potential error in heat-flow values arising from the estimated thermal-conductivity values would be reduced by averaging over several intervals, each of which is several hundred metres thick (Majorowicz et al., 1995).

Majorowicz et al. (1995) used average values for the thermal conductivity of rocks at 20°C and net rock data determined from geological well logs for 1000 ft. (304.8 m) intervals to determine the effective conductivity for the depth interval between the base of ice-bearing permafrost and the bottom of the well for 188 wells in the Mackenzie Delta–Beaufort Sea region. This approach, however, does not consider the

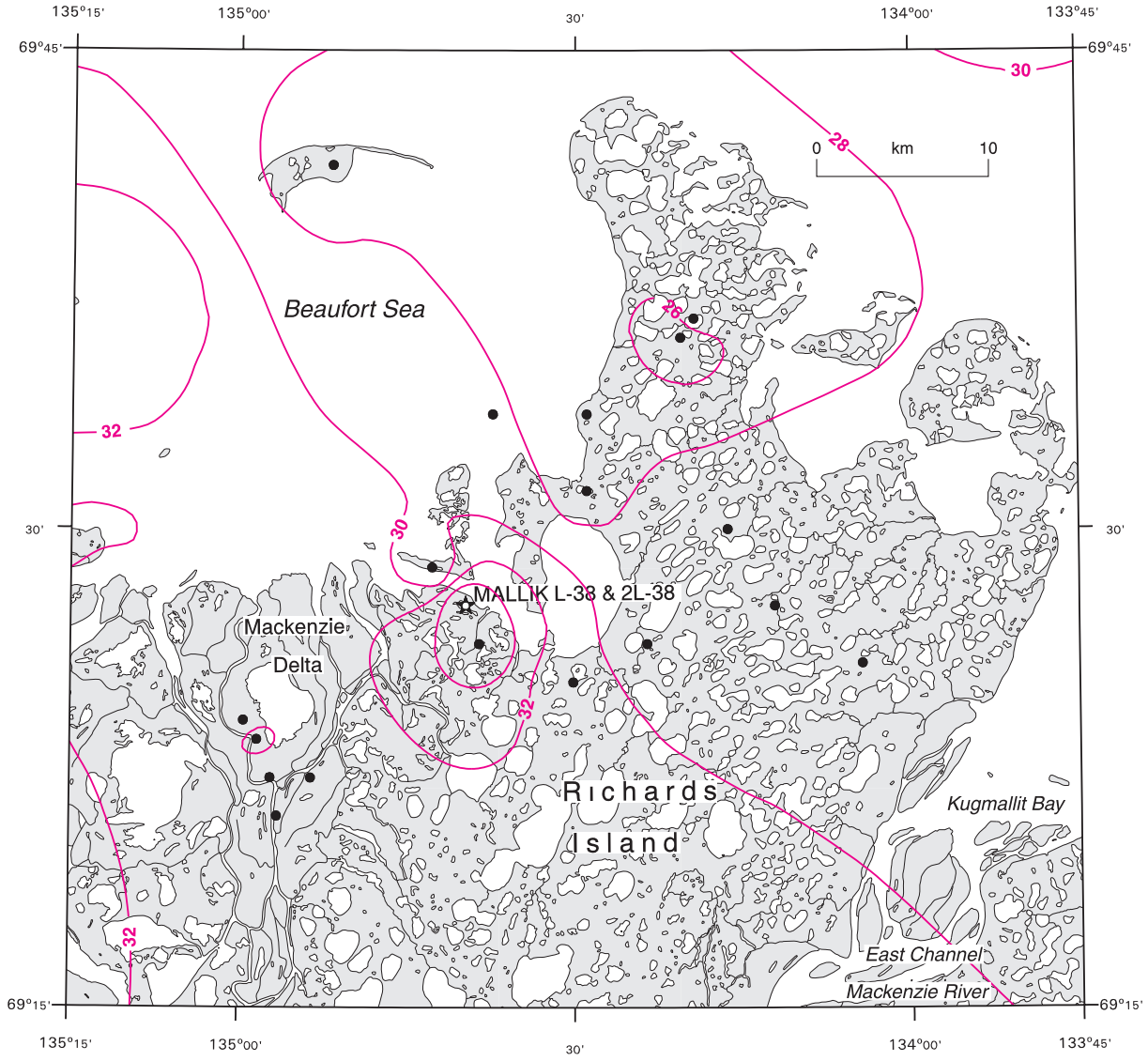

Figure 3. *Average geothermal gradient (K/km) based on the least-squares fit to the corrected industrial temperature data and constrained by the -1°C isotherm at the ice-bearing permafrost base. The isoline interval is 2 K/km.*

dependency of thermal conductivity on porosity and, therefore, depth, nor does it consider the variation of thermal conductivity with formation temperature. The present study takes these factors into account in the determination of effective thermal conductivity.

Issler (1995) determined the relationship between shale and sandstone porosity and depth for the Mackenzie Delta–Beaufort Sea region. The thickness of the eroded overburden is assumed to be 400 m. These relationships are used in this study to estimate the porosity for each interval. If the porosity is known, the water-saturated rock thermal conductivity can be calculated as the geometric mean from the solid and pore-fluid thermal conductivities weighted according to their fractional volumes (Chapman et al., 1984). The thermal conductivity of pore fluid is assumed to be 0.6 W/m·K. Sandstone and shale are the major contributors to the basin sedimentary fill (Majorowicz et al., 1995) and their thermal conductivities (at 20°C) are assumed to be 4.5 W/m·K and 2.5 W/m·K respectively. The thermal conductivity of the solid matrix component is assumed to be inversely proportional to the formation temperature and the equation given by Chapman et al. (1984) was used to adjust the thermal-conductivity values at 20°C to the in situ conditions.

Calculated thermal-conductivity values and the associated error for 1000 ft. (304.8 m) intervals for the 19 wells in the mapped area and the 13 wells in the immediate vicinity are given in an unpublished report by ASL Environmental Sciences Inc. (1998). The error is generally in the range of 15–20% but can be as high as 35%.

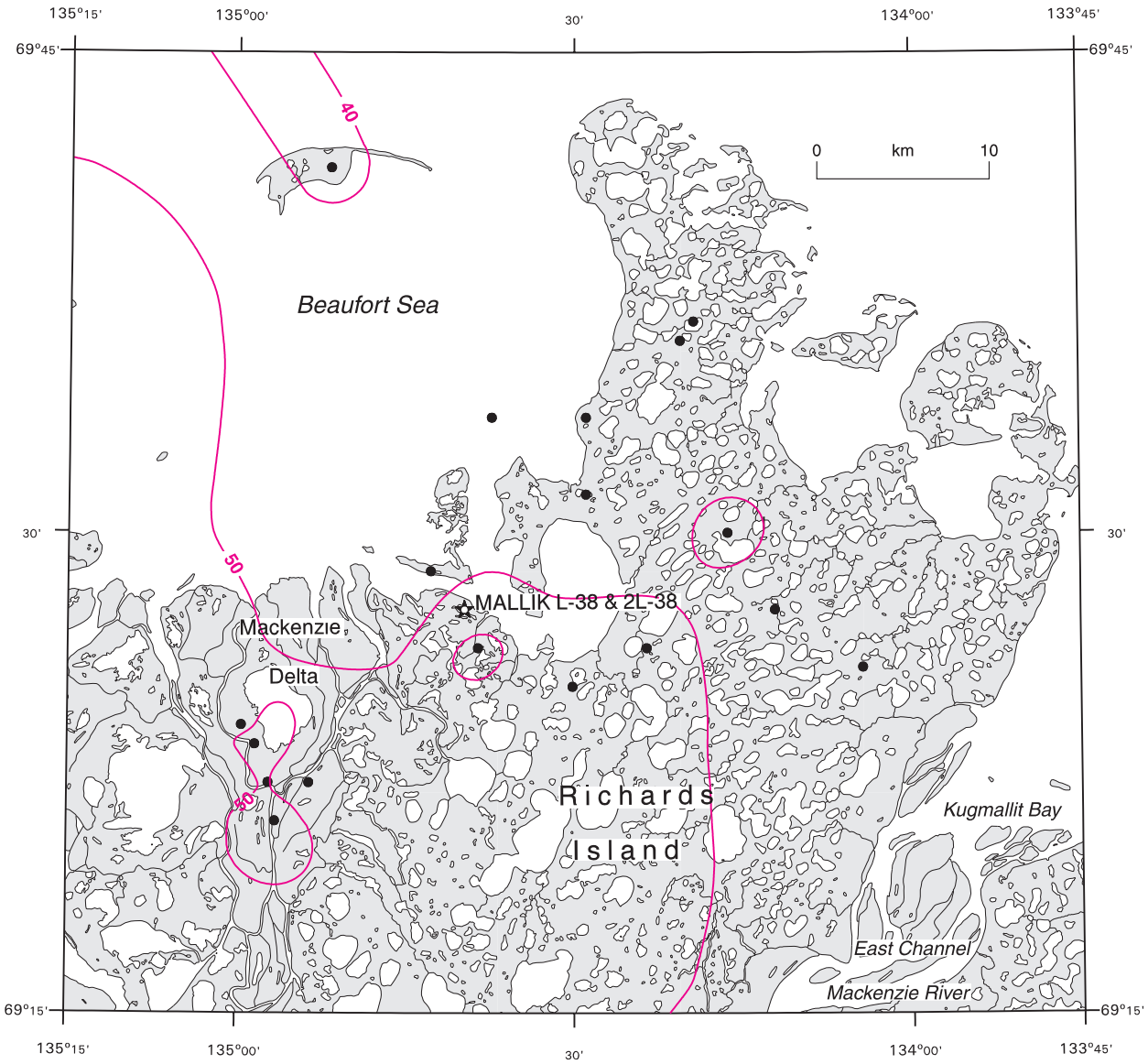

Figure 4. *Estimated heat flow (mW/m^2) in the Mallik field area. The isoline interval is 10 mW/m^2.*

Heat flow was determined for each well using equation 1 with the thermal gradient values given in Table 1 and the effective thermal conductivity calculated from equation 2. The heat-flow values for the 32 wells are also given in Table 1. The spatial variation in heat flow is shown in Figure 4. The error of heat-flow estimates can be as high as 20% and is largely due to errors in thermal-conductivity estimates. Heat flow ranges from 39 mW/m^2 to 55 mW/m^2 in the mapped area. Heat flow is as high as 61 mW/m^2 just to the west of the mapped area (Table 1). Heat-flow variations less than 10 mW/m^2 are close to the error of the heat-flow estimate and are, therefore, insignificant. There does, however, appear to be a southwestward increase in heat flow (Fig. 4).

Reconstruction of temperature-depth profiles

The temperature-depth profiles beneath the base of ice-bearing permafrost were reconstructed for the 32 wells using the following (Majorowicz et al., 1990):

$$T(z)= T_o + Q\Sigma(dz/k) \quad (3)$$

where z is depth (m), Q is heat flow (W/m^2), T_o is the temperature at the base of ice-bearing permafrost (assumed to be -1°C), and k is the thermal conductivity (W/m·K) for the interval dz. Intervals 1000 ft. (304 m) thick were used in the calculations and average values of thermal conductivity (determined as described in previous section) were assigned to each interval. An example of a theoretically reconstructed temperature-depth profile for the Mallik L-38 well is shown in Figure 5. The reconstructed temperature-depth profile is the best estimate of the equilibrium temperature condition in the well. The reconstructed temperature-depth profile for each well and the numerical values (excluding permafrost zone) are summarized in an unpublished report by ASL Environmental Sciences Inc. (1998).

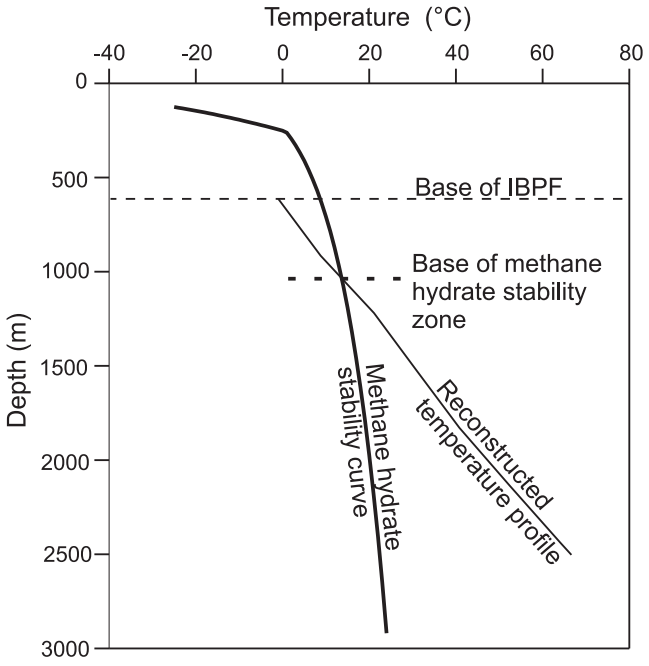

Figure 5. *Theoretically reconstructed temperature-depth profile determined from equation 3 for the Mallik L-38 well superimposed on the methane hydrate stability curve. The area to the left of the stability curve represents conditions for gas hydrate stability. Base of IBPF refers to the base of the ice-bearing permafrost.*

Regional temperature field

The reconstructed temperature-depth profiles were used to determine the temperature at two depths, 3000 ft. (915 m) and 5000 ft. (1524 m). The regional variation in temperature at these two depths is shown in Figure 6a and Figure 6b. The depth to the -1°C isotherm which represents the base of ice-bearing permafrost has also been mapped (Fig. 7). Higher temperatures at depth and thinner permafrost are found in the southwest corner of the mapped region. Permafrost is substantially thinner to the west of the mapped region (Table 1) where it is only 67 m thick.

The small regional variations of heat flow and effective thermal conductivity can account for some of the variation in subsurface temperature but the surface temperature history in this region is likely also an important factor. The sediments of the eastern Mackenzie Delta and the adjacent Beaufort Shelf were exposed to low air temperatures during the Wisconsinan Glaciation due to the absence of glacial ice or a recession of seawater. Thick permafrost was able to form in these areas as shown in Figure 7. In areas west of about 135°W, ice sheets insulated the ground from the low temperatures of the Wisconsinan Glaciation and thick permafrost could not develop (Judge et al., 1987).

DEPTH TO THE BASE OF METHANE HYDRATE STABILITY ZONE

Gas hydrate stability is dependent on temperature and pressure. Gas composition is also an important factor but only the stability of methane hydrate is considered in this study because the dominant gas in the Mackenzie Delta–Beaufort Sea region is methane (Davidson et al., 1978). The temperature-pressure conditions for methane (Structure I) hydrate stability are described by the following equations (Holder and Hand, 1982; Collett, 1993):

$$P(kPa)= \exp(14.7170-1886.79/TK) \text{ from 248 to 273 K or -25°C to 0°C} \quad (4)$$

$$P(kPa)= \exp(39.9803-8533.80/TK) \text{ from 273 to 298 K or 0°C to 25°C} \quad (5)$$

where TK is temperature in Kelvin and P(kPa) is the formation pressure. If hydrostatic pressure conditions are assumed, the temperature required for methane hydrate stability at a given depth can be determined as shown in Figures 2 and 5.

Previous studies (Judge and Majorowicz, 1992; Judge et al., 1994) have analyzed the conditions for gas hydrate stability in the Mackenzie Delta–Beaufort Sea region by superimposing the linear temperature profile determined for each well on the methane hydrate stability curve as shown in Figure 2. The maximum depth of the methane hydrate stability zone is determined by calculating the depth of the intersection of the stability curve and the ground temperature profile. The depth to the base of the methane hydrate stability zone using this method is given in Table 1 for the 32 wells studied. The error associated with these estimates can be ±150 m and is due mainly to uncertainties in the correction of bottom-hole-temperature and drill-stem-temperature data and in the variations of thermal conductivity with depth. The use of temperature-depth data based on the least-squares linear fit to evaluate the gas hydrate stability conditions is therefore only a first-order approximation because variations in thermal conductivity throughout the sedimentary section are not considered.

In order to improve the estimates of the depth to the base of the methane hydrate stability zone, the reconstructed temperature-depth curve (calculated using equation 3) for each well was superimposed on the methane hydrate stability curve and the intersection of the two curves was determined

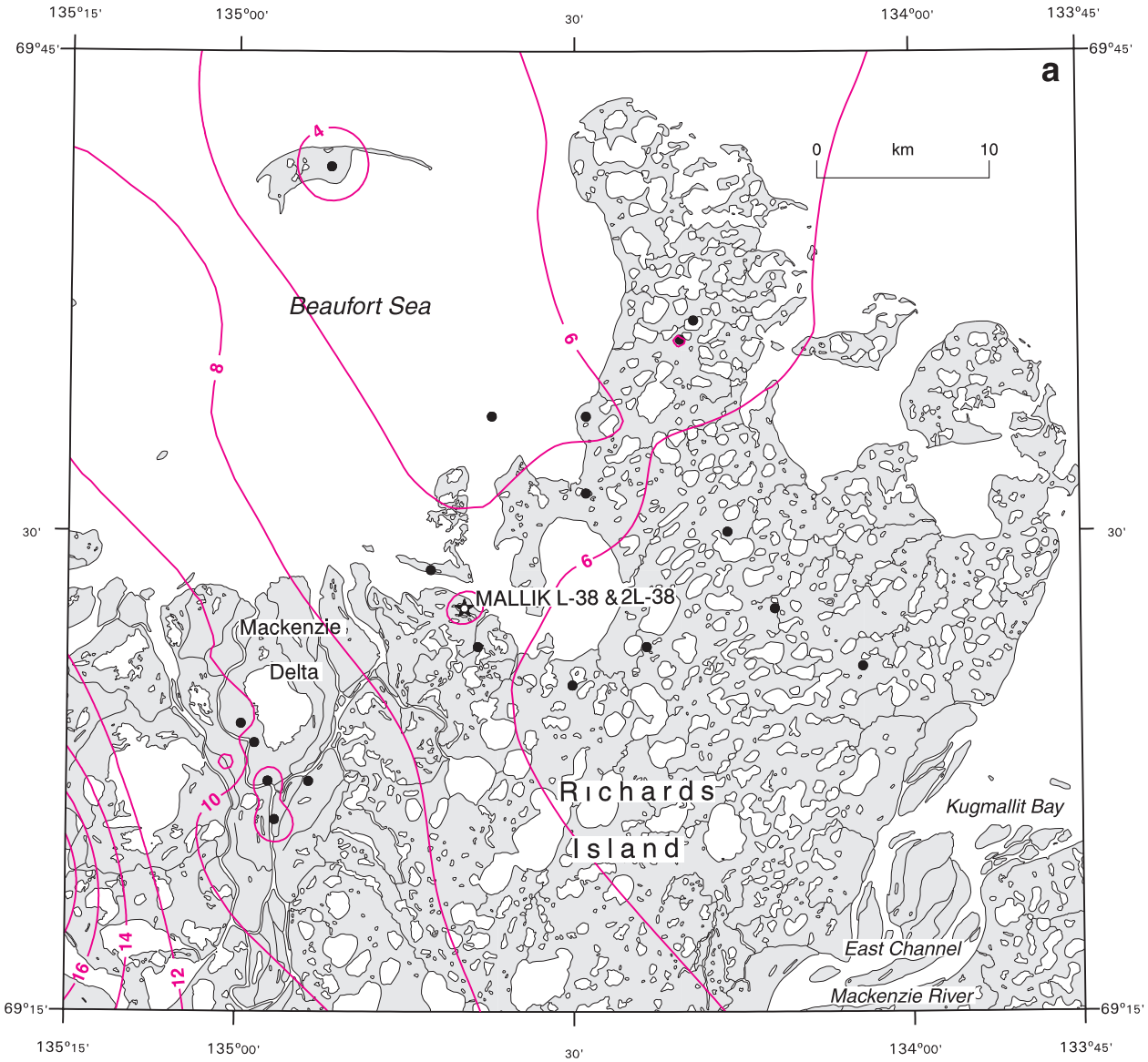

Figure 6. *Temperature (°C) distribution at two depth levels;* ***a)*** *3000 ft. (900 m);* ***b)*** *5000 ft. (1500 m). The isotherm interval is 2°C and 5°C for Figures 6a and 6b, respectively.*

(Fig. 5). The depth to the base of the methane hydrate stability zone determined using the reconstructed temperature-depth profiles for the 32 wells is also given in Table 1. For 19 of the wells, the base of the stability zone is 50–150 m deeper than that determined using linear temperature profiles (Table 1). Similar results were obtained from both methods for eight wells while the reconstructed temperature-depth profiles yielded a 50–100 m shallower base for five of the wells.

The regional variation in the depth to the base of the methane hydrate stability zone determined using the reconstructed temperature-depth profiles is shown in Figure 8. Conditions for methane hydrate stability exist over the entire area shown in Figure 8, but methane hydrate is unstable to the west of this region where permafrost is less than 200 m thick. Within the mapped area, the base of the methane hydrate stability zone varies from about 1000 m to 1500 m deep. The base of the methane hydrate stability zone is shallower in the southwest portion of the study region where thinner permafrost is found. In the Mallik field area the depth to the base of the stability zone is about 1200 m.

The depth to the top of the methane hydrate stability zone is estimated to be 220 ± 10 m. This value, along with the depth to the base of the stability zone, estimated using reconstructed temperature-depth profiles, was used to calculate the thickness of the methane hydrate stability zone (Table 1). The methane hydrate stability zone may be as thick as 1200 m in

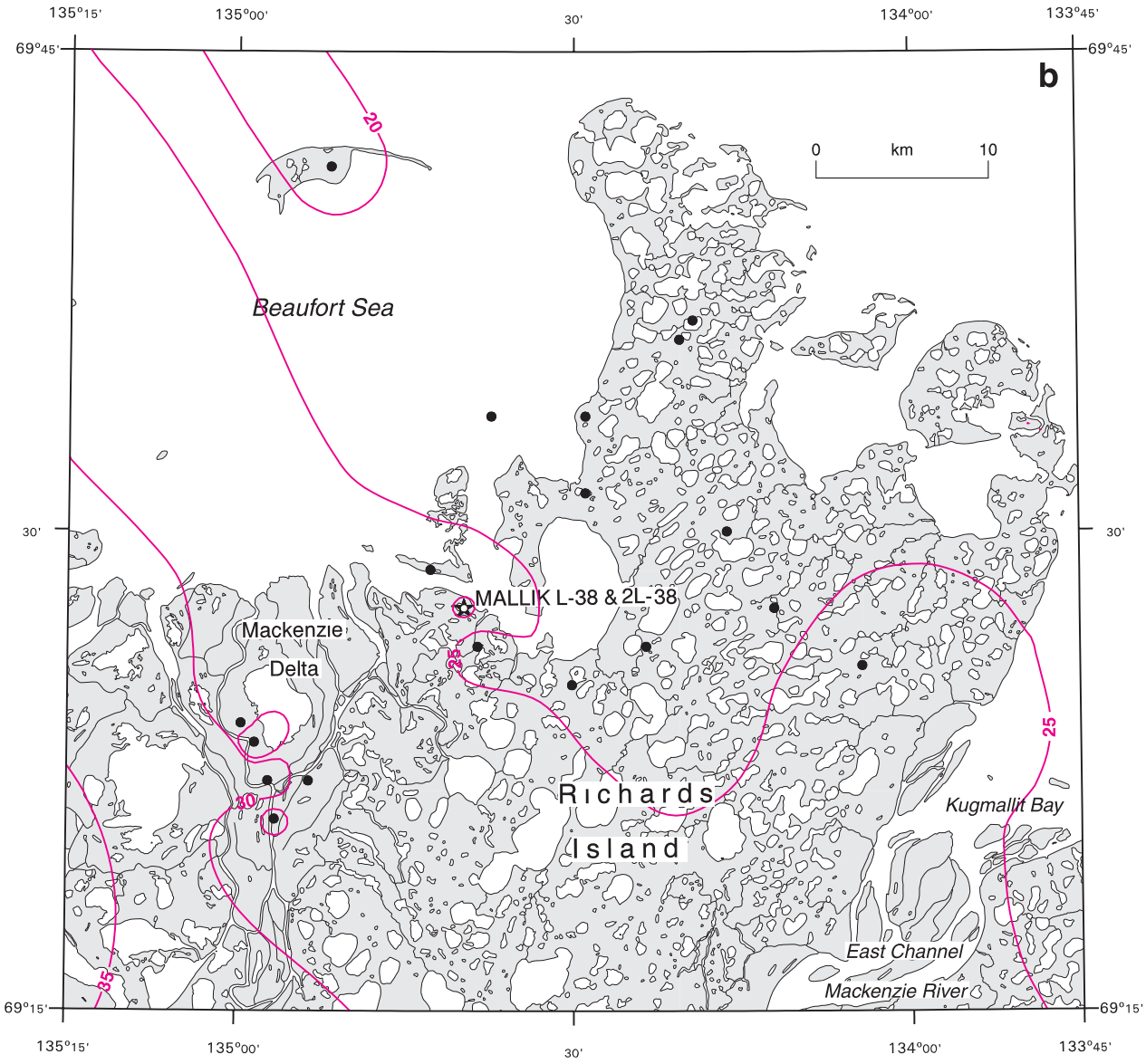

Figure 6b.

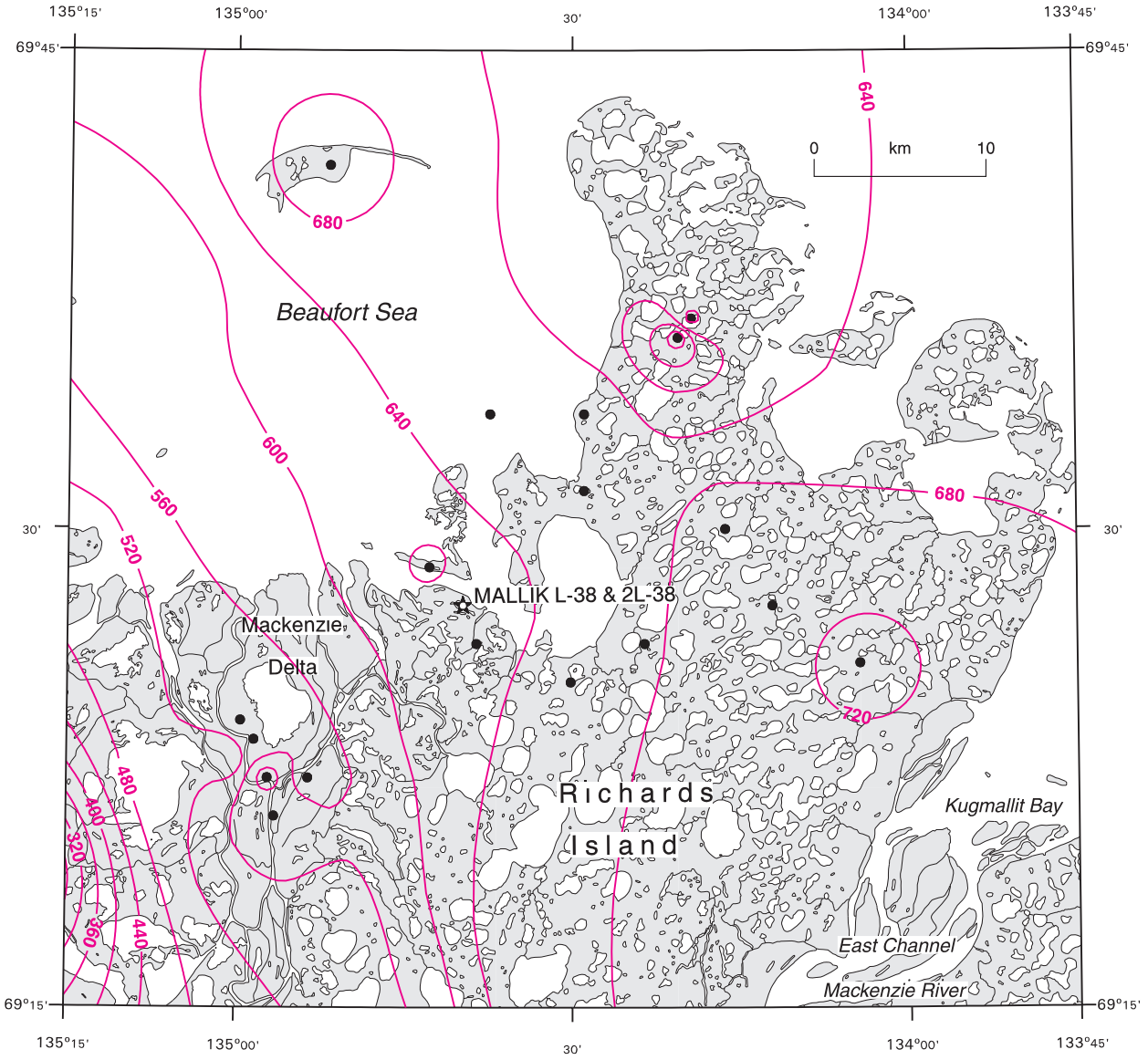

Figure 7. *Depth to the base of ice-bearing permafrost (in metres below the surface level). The isoline interval is 40 m.*

areas where permafrost is greater than 600 m thick. Where permafrost thickness is less than 600 m, such as in the south-west portion of the study area, the methane hydrate stability zone is less than 800 m thick.

CONCLUSIONS

This study has attempted to improve estimates of heat-flow and temperature-depth profiles in the Mallik field area by refining the thermal-conductivity values used to make the estimates. The reconstructed temperature-depth profiles have been used to assess the stability conditions for methane hydrate. Methane hydrate is stable throughout the region shown in Figure 8 but conditions for gas hydrate stability do not exist to the west of this area where permafrost is less than 200 m thick. The depth to the base of the methane hydrate stability zone is greater than 1000 m in most of the study region and the methane hydrate stability zone can be greater than 1000 m thick in areas underlain by thick permafrost. The base of the gas hydrate stability zone is 1200 ± 100 m in the Mallik field area which is in good agreement with the results of the new Mallik 2L-38 well gas hydrate study (*see* Wright et al., 1999). The spatial variation in the thickness of permafrost and the gas hydrate stability zone are partly controlled by the small variations in geothermal gradient and heat flow. Other factors, however, such as the surface temperature history related to, for example, climate change or sea-level changes,

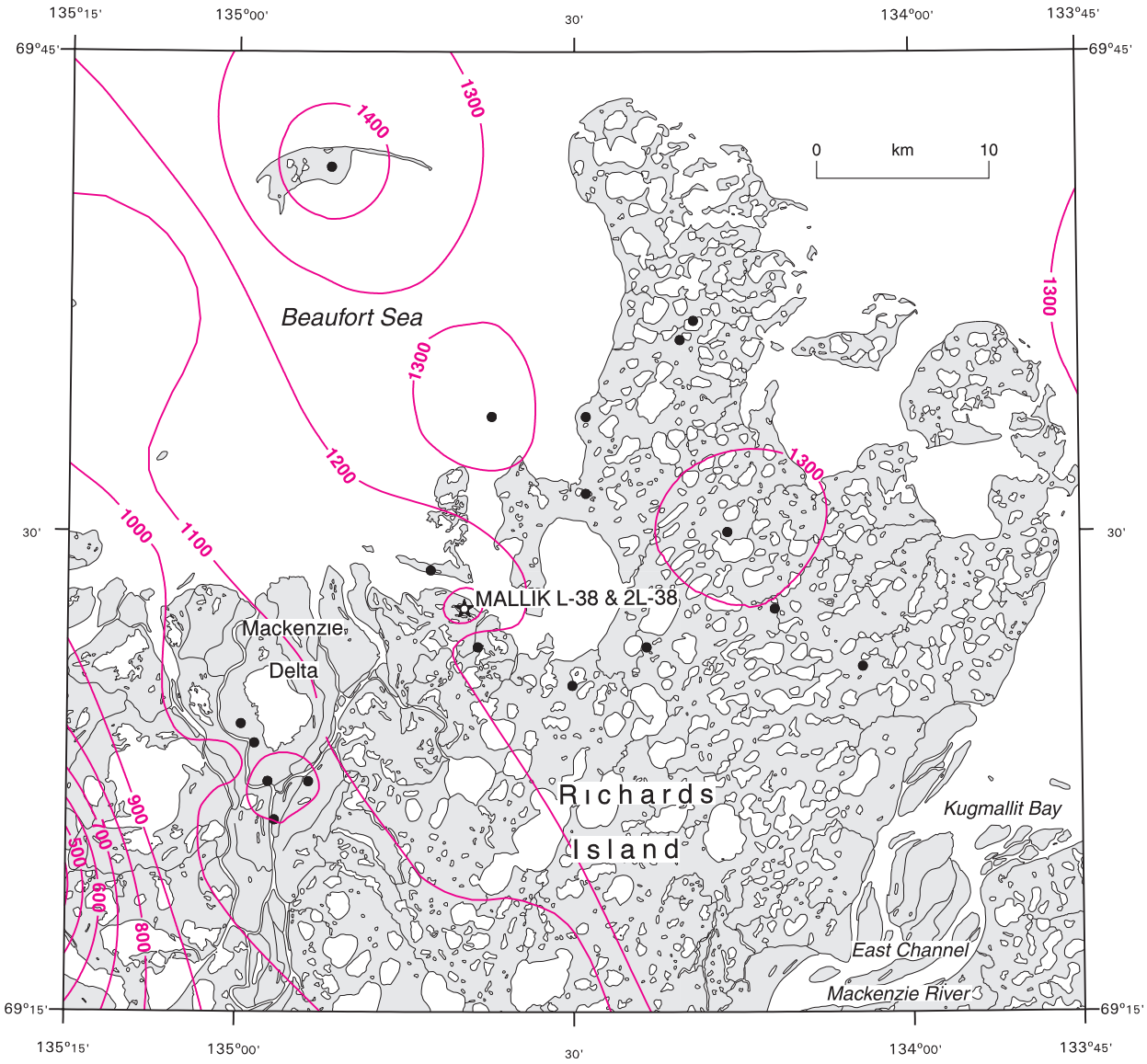

Figure 8. *Depth to the base of the methane hydrate stability zone (in metres below the surface level). The isoline interval is 100 m.*

also control the regional distribution of permafrost and hence the thickness of the gas hydrate stability zone (*see* Taylor, 1999).

For a majority of the wells, the base of the methane hydrate stability zone determined using the reconstructed temperature-depth profiles is 50–150 m deeper than that estimated by Judge and Majorowicz (1992) using the linear temperature profiles. This difference becomes important when evaluating the potential hazard that gas hydrate may pose during drilling. The results of this study show that an accurate assessment of the thermal properties and the subsurface temperature field are required to provide reliable estimates of the areal and vertical extent of the gas hydrate stability zone and the size of the gas hydrate reservoir.

ACKNOWLEDGMENTS

This contribution was funded by the Geological Survey of Canada (scientific authority - Scott Dallimore) through a PWGSC contract to ASL Environmental Sciences Inc. J. Majorowicz would like to thank Scott Dallimore, ASL Environmental Sciences Inc., and Al Taylor for help with the subcontract. Comments on the manuscript by Al Taylor, Margo Burgess, and two anonymous reviewers are appreciated. A. Prégent of the Terrain Sciences Division of GSC produced the maps.

REFERENCES

Chapman, D.S., Keho, T.H., Bauer, M.S., and Picard, M.D.
1984: Heat flow in the Uinta Basin determined from bottom hole temperature (BHT) data; Geophysics, v. 49, no. 4, p. 453–466.

Collett, T.S.
1993: Natural gas hydrates of the Prudhoe Bay and Kuparuk River area, North Slope, Alaska; The American Association of Petroleum Geologists Bulletin, v. 77, no. 5, p. 793–812.

Collett, T.S. and Dallimore, S.R.
1998: Quantitative assessment of gas hydrates in the Mallik 2L-38 well, Mackenzie Delta, N.W.T.; *in* The 7th International Permafrost Conference Proceedings; Université Laval, Collection Nordicana, no. 57, p. 189–194.

D&S Petrophysical Consultants
1983: A study of well logs in the Mackenzie Delta/Beaufort Sea to outline permafrost and gas hydrate occurrence; Energy Mines and Resources Canada, Earth Physics Branch, Open File 83-10.

Dallimore, S.R. and Collett, T.S.
1998: Gas hydrates associated with deep permafrost in the Mackenzie Delta N.W.T., Canada: regional overview; *in* The 7th International Permafrost Conference Proceedings; Université Laval, Collection Nordicana, no. 57, p. 201–206.

Davidson, D.W., El-Defrawy, M.K., Feuglem, M.O., and Judge, A.S.
1978: Natural gas hydrates in northern Canada; *in* Proceedings of Third International Conference on Permafrost, v. 1, p. 937–943.

Holder, G.D. and Hand, J.H.
1982: Multiple-phase equilibrium in hydrates from methane, ethane, propane, and water mixtures; Journal American Institute of Chemical Engineers, v. 28, no. 3, p. 440–447.

Issler, D.
1995: Compaction and Subsidence; *in* Geological Atlas of the Beaufort-Mackenzie Area, (ed.) J. Dixon; Geological Survey of Canada, Miscellaneous Report 59, p. 136–143.

Judge, A.S. and Majorowicz, J.A.
1992: Geothermal conditions for gas hydrate stability in the Beaufort-Mackenzie area: the global change aspect; Global and Planetary Change, v. 98, no. 2/3, p. 251–263.

Judge, A.S., Pelletier, B.R., and Norquay, I.
1987: Permafrost base and distribution of gas hydrates; *in* Marine Science Atlas of the Beaufort Sea, (ed.) B.R. Pelletier; Geological Survey of Canada, Miscellaneous Report 40, p. 39.

Judge, A.S., Smith, S.L., and Majorowicz, J.A.
1994: The current distribution and thermal stability of natural gas hydrates in the Canadian Polar regions; *in* Proceedings IVth International Offshore and Polar Engineers Conference, Osaka, Japan, The International Society of Offshore and Polar Engineers, v. 1 p. 307–314.

Majorowicz, J.A., Jessop, A., and Judge, A.S.
1995: Geothermal regime, maps; *in* Geological Atlas of the Beaufort-Mackenzie area (ed.) J. Dixon; Geological Survey of Canada, Miscellaneous Report 59, p. 33–37.

Majorowicz, J.A., Jones, F.W., and Judge, A.S.
1990: Deep subpermafrost thermal regime in the Mackenzie Delta basin, northern Canada — Analysis from petroleum bottom-hole temperature data; Geophysics, v. 55, no. 3, p. 362–371.

Smith, S.L. and Judge, A.S.
1993: Gas hydrate database for Canadian Arctic and selected East Coast wells; Geological Survey of Canada, Open File 2746, 120 p.

Taylor, A.E.
1999: Modelling the thermal regime of permafrost and gas hydrate deposits to determine the impact of climate warming, Mallik field area; *in* Scientific Results from JAPEX/JNOC/GSC Mallik 2L-38 Gas Hydrate Research Well, Mackenzie Delta, Northwest Territories, Canada, (ed.) S.R. Dallimore, T. Uchida, and T.S. Collett; Geological Survey of Canada, Bulletin 544.

Taylor, A.E. and Judge, A.S.
1981: Measurement and prediction of permafrost thickness, Arctic Canada; *in* Technical Papers, 51st Annual Meeting, Society of Exploration Geophysicists, v. 6, p. 3964–3977.

Taylor, A.E., Burgess, M., Judge, A.S., and Allen, V.S.
1982: Canadian geothermal data collection — northern wells 1981; Energy, Mines and Resources Canada, Earth Physics Branch, Geothermal Series No. 13, 153 p.

Wright, J.F., Dallimore, S.R., and Nixon, F.M.
1999: Influences of grain size and salinity on pressure-temperature thresholds for methane hydrate stability in JAPEX/JNOC/GSC Mallik 2L-38 gas hydrate research well sediments; *in* Scientific Results from JAPEX/JNOC/GSC Mallik 2L-38 Gas Hydrate Research Well, Mackenzie Delta, Northwest Territories, Canada, (ed.) S.R. Dallimore, T. Uchida, and T.S. Collett; Geological Survey of Canada, Bulletin 544.